IMAGING FLAWS UNDER INSULATION USING A SQUID MAGNETOMETER

A. C. Bruno, C. Hall Barbosa, J. E. Zimmerman,
P. Costa Ribeiro, E. Andrade Lima, L. F. Scavarda,
C. Kelber, J. Szczupak[1], and C. S. Camerini[2]
Department of Physics and [1]Department of Electrical Engineering
Pontifical Catholic University of Rio de Janeiro
Rua Marquês de São Vicente 225, Rio de Janeiro, RJ 22453-900, Brazil
[2]CEMEC-CENPES, PETROBRÁS

INTRODUCTION

Superconducting QUantum Interference Devices (SQUID) are the most sensitive instruments known for the measurement of magnetic fields. An all niobium two-hole home-made SQUID can easily achieve sensitivities of $10^{-4}\ \Phi_0/\sqrt{Hz}$ ($\Phi_0 = 2.07 \times 10^{-15}$ Wb). Our complete system has a sensitivity of 50×10^{-15} Tesla $/\sqrt{Hz}$, and more sophisticated systems can reach sensitivities one order of magnitude higher. Due to its high sensitivity, and to the advent of high temperature superconductivity, SQUID systems presents new opportunities for its use in nondestructive evaluation of electrically conducting and ferromagnetic structures, mainly when the area to be inspected is difficult to be reached.

The detecting scheme consists of applying an electric current to the sample and measuring the magnetic response. If a flaw is present, it will distort the field near it. SQUIDs are usually used with a set of coils wound in a gradiometric configuration, in order to be insensitive to the large environmental magnetic fields usually present at the measurement site. In many situations, the signal due to the flaw is immersed in another background field due to the sample excitation scheme, whether field or current is used. When current is injected in a flawed plate, if the sensor is at a relatively large distance from the plate, the signal generated by the flaw is masked by the signal generated by the unflawed portions of the plate. This results in a ramp-shaped signal. The same happens if a magnetic signal is induced on a defective ferromagnetic plate. If the surface of the plate is not perfectly parallel with the gradiometer coil plane, as the magnetometer is scanned over it, a magnetic field ramp is generated, masking the signal due to the flaw.

A portable home-made SQUID magnetometer was used in nondestructive evaluation of metallic plates. We were able to image flaws in plates with thermal insulation up to 9 cm thick. We used two-dimensional digital FIR filters to enhance the magnetic field disturbance due to the flaw. Without filtering, visual inspection is difficult when the distance from the system to the flaw exceeds 5 times its size. Applying the enhancement algorithm, magnetic field disturbances could be visualized at distances 10 times the size of the flaw.

Review of Progress in Quantitative Nondestructive Evaluation, Vol. 15
Edited by D.O. Thompson and D.E. Chimenti, Plenum Press, New York, 1996

THE SQUID SYSTEM

We have constructed a number of RF-biased niobium point-contact SQUID's for use in a magnetometer system [1]. They are essentially the same to those introduced in 1970 and produced commercially for several years [2], except for a simplified design of the point contact. In place of the pair of tiny screws and lock-nuts, we used a pair of niobium wire segments held by friction in a closely fitting hole. This SQUID is affordable for any laboratory having a simple machine shop.

Due to its very high sensitivity, the SQUID must be used together with a flux transformer. The flux transformer consists of a primary coil wound in a gradiometric configuration and a secondary coil inductively coupled to the SQUID. The gradiometer consists of coaxial coils connected in series and separated by a distance called baseline (Figure 1). It works as a spatial differentiator, favoring fields from near sources against fields from distant ones. As the noise sources are located far from the gradiometer, the spatial distribution of the magnetic field due to them will have, in a Taylor series expansion, only the constant and perhaps the first derivative components. A second order gradiometer will cancel both components allowing the magnetic field due to the near but weaker source to be detected. We used a second order gradiometer with 1.5 cm diameter coils and 4 cm baseline, both immersed in a liquid helium container.

A schematic drawing of the complete system is shown in Figure 2. The Dewar is made of fiberglass, and superinsulation material was used to isolate the inner and outer cans. The overall Dewar size is 15 cm in diameter and 40 cm in height. The system needs pre-cooling with liquid nitrogen for 2 hours before liquid helium transfer. Dewar capacity is 2 liters and it holds helium for about 24 hours.

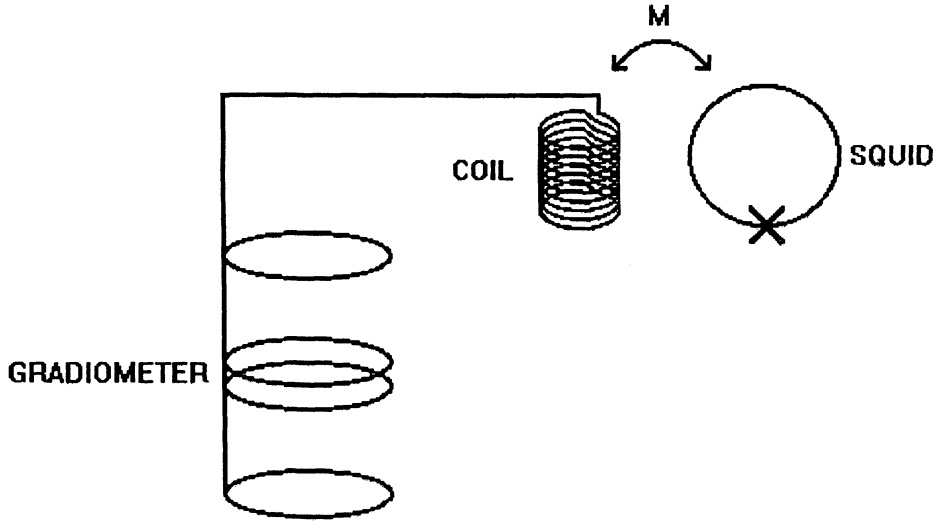

Figure 1. Schematic view of the SQUID coupled to a flux transformer consisting of a second order gradiometer and a secondary coil. The diameter of each coil is 1.5 cm and the distance between each set of coils is 4 cm.

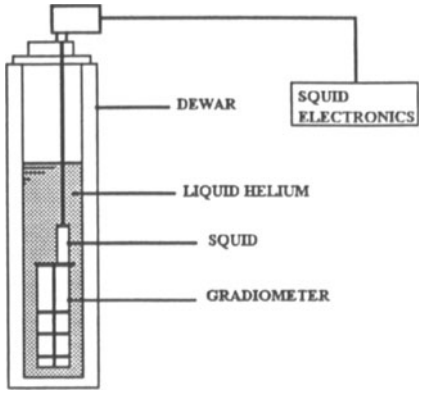

Figure 2. SQUID system consisting of the SQUID sensor, gradiometer, liquid helium dewar and electronics.

BIDIMENSIONAL FILTERING AND RESULTS

Figure 3 shows an image representation of the magnetic field B_z generated by a 1m x 1m x 1mm aluminum plate with an 8 mm hole, carrying 5 A current. Each level of gray corresponds to a different value of the detected magnetic field. Black corresponds to the minimum field and white to the maximum. The signal was detected by our SQUID system at a 9 cm standoff distance. Because the sensor is at a large distance from the plate, the signal generated by the flaw is masked by the signal generated by the unflawed portions of the plate. Instead of the well-known dipolar pattern, the result is a monotonic increase of the magnetic field signal as we scan the plate perpendicularly to the direction of the applied current.

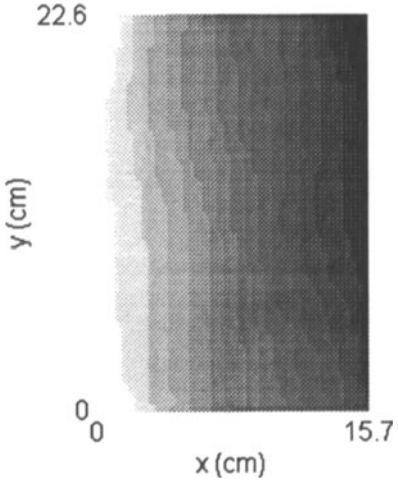

Figure 3. Image representation of the magnetic field generated by an 1m x 1m x 1mm aluminum plate with an 8 mm hole in the center, carrying 5 A current. Each level of gray corresponds to a different value of the detected magnetic field. The signal was detected by our SQUID system at a 9 cm standoff distance. The image has been displayed to present maximum dynamic range.

In order to get rid of the signal generated by the plate, we must use a high-pass spatial filter. This filter is implemented by low-pass filtering the image with a high-order FIR filter and then subtracting the result from the original image. This is a modified version of an image enhancement procedure called *unsharp masking* [3]. We need also to use a low-pass filter to clean the image from the environmental white noise present at the measurement site.

The filters we implemented are based on spatial operations performed on local neighbors of input pixels (field values). The image is convolved with a finite impulse response filter called a *spatial mask*. Each pixel is replaced by a weighted average of its neighborhood pixels, that is:

$$b(m,n) = \sum_{(k,l)\in W}\sum \beta(k,l)\cdot a(m-k,n-l) \qquad (1)$$

where $a(m,n)$ e $b(m,n)$ are the input and output images of the filter, respectively, W is the window defining the spatial mask and $\beta(k,l)$ are the filter coefficients. The spatial mask used for the low-pass filter is shown below:

0	$\frac{1}{16}$	0
$\frac{1}{16}$	$\frac{3}{4}$	$\frac{1}{16}$
0	$\frac{1}{16}$	0

m

n

The criterion for choosing the low-pass filter order is based on the overall signal-to-noise ratio improvement. This will depend on the distance from the plate and on the environmental magnetic noise. For our system we used low-pass filter orders in the range from 10 to 20. This corresponds to applying the above mask 10 to 20 times over the magnetic image. This spatial mask was chosen so as to allow a fine control over the low-pass filtering process.

The criterion for choosing the high-pass filter order is based on experimental observations to ensure that the image is free from the background field due to the sample excitation scheme. It was observed that for filter orders above 80 there was no noticeable enhancement on the final result. The low-pass spatial mask used in the high-pass filtering procedure is shown below:

$\frac{1}{9}$	$\frac{1}{9}$	$\frac{1}{9}$
$\frac{1}{9}$	$\frac{1}{9}$	$\frac{1}{9}$
$\frac{1}{9}$	$\frac{1}{9}$	$\frac{1}{9}$

m

n

The technique used to avoid distortions on the image borders due to the filtering process is based on a mirroring procedure [4]. Figure 4 shows the result of the filtered data, where the characteristic dipolar pattern can be easily observed.

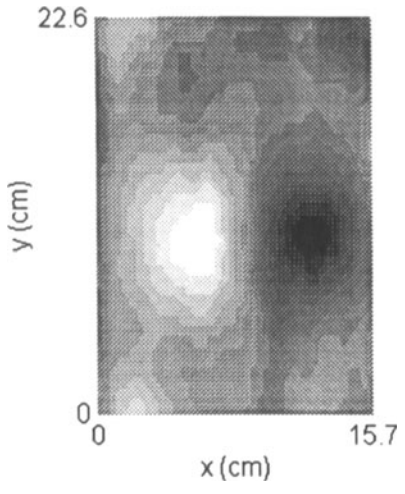

Figure 4. Image from Figure 3 processed by a 20th order low-pass filter followed by a 80th order high-pass filter. The image has been displayed to present maximum dynamic range.

This procedure was tested successfully on a number of situations with aluminum plates having holes in the center with diameters ranging from 2 mm to 8 mm, with currents varying from 100 mA to 5 A and at standoff distances from 1.5 cm to 9 cm. The data were taken in a harsh laboratory environment.

CONCLUSION

A low-cost SQUID magnetometer was built to be used in nondestructive evaluation of metallic structures. We used image processing techniques to enhance the visualization of the magnetic data. The process consisted of high-pass filtering the data to remove the signal due to the unflawed portions of the plate. Further a low-pass filter is used with the filter order depending on the sample distance and background noise. Applying this algorithm, magnetic field disturbances could be visualized at distances greater than 10 times the diameter of the flaw.

ACKNOWLEDGMENTS

This work was partially supported by CNPq, RHAE, FINEP and PETROBRÁS.

REFERENCES

1. A. C. Bruno and J. E. Zimmerman, *Superconducting Devices and Their Applications,* eds. H. Koch and H. Lübbig (Springer-Verlag, Berlin, 1992), p. 240.
2. J. E. Zimmerman, P. Thiene and J. T. Harding, J. Appl. Phys. 41, 1572 (1970).
3. A. K. Jain, *Fundamentals of Digital Image Processing,* (Prentice-Hall, New York, 1989).
4. M. J. T. Smith and S. L. Eddins, IEEE Trans. ASSP 38, 1446 (1990).